Journal of the Ceramic Society of Japan 133 [7] 389-392 2025
DOI https://doi.org/10.2109/jcersj2.25048

JCS-Japan

FULL PAPER

Preparation and photoluminescence of Eu^{2+} and Eu^{3+}-doped $NaLuO_2$

Hisanori Yamane[1,†], Akihiro Nakanishi[1], Shiro Funahashi[1], Takayuki Nakanishi[1], Kohsei Takahashi[1], Naoto Hirosaki[1] and Takashi Takeda[1,‡]

[1] Advanced Phosphor Group, National Institute for Materials Science, Tsukuba, Ibaraki 305–0044, Japan

Single phase $NaLuO_2$, which crystallizes in the α-$NaFeO_2$-type structure (trigonal, space group $R\bar{3}m$), was synthesized by heating a mixture of Na_2O and Lu_2O_3 at 1150 °C. The crystal structure of this oxide was analyzed using the Rietveld method for the powder X-ray diffraction pattern, and the oxygen atom coordinate [z = 0.2397(3)] was refined. Mixtures of $NaLuO_2$ and europium monoxide with a composition $NaLuO_2$–xEuO (x = 0.0, 0.01, 0.1, 1.0 mol %) were heated at 900 °C for 12 h in a N_2 atmosphere. The obtained samples were Eu^{2+} and Eu^{3+}-doped $NaLuO_2$ with trace amounts of Lu_2O_3. The emission spectrum peak due to the $5d \rightarrow 4f$ transition of Eu^{2+} occurred at a wavelength of 617 nm under the excitation of a 442 nm blue light, and the full width at half maximum of the spectrum was 80 nm. Intense emission peaks due to the f-f transition of Eu^{3+} were observed at approximately 590 nm when excited by a 230 nm ultraviolet light.

Key-words : Solid state reaction, Ternary oxide, Powder X-ray diffraction, Rietveld analysis, Photoluminescence, Eu^{2+} and Eu^{3+} emission center

[Received March 28, 2025; Accepted April 11, 2025]

1. Introduction

Considering potential applications for X-ray scintillators and white LED lighting, Jarý et al. have been actively investigating the fluorescent properties of Eu^{2+}-doped trinary sulfides ($ALnS_2$, A = Na, K, Rb; Ln = La, Gd, Lu, Y) with the α-$NaFeO_2$-type structure (trigonal, space group $R\bar{3}m$).[1–8] Ternary oxides with the α-$NaFeO_2$-type structure consisting of alkali metals and rare-earth elements have also been synthesized,[9–14] and the fluorescent properties of Eu^{3+} or Bi^{3+}-doped ones have been previously reported.[14–16] Additionally, research has also been conducted on the magnetic properties of $ALnO_2$ (A = Na; Ln = Er, Tm, Yb, Lu, A = K; Ln = Y, Nd, Sm–Lu).[17,18]

An emission peak of 0.05 % Eu^{2+}-doped ternary sulfide $NaLuS_2$ with the α-$NaFeO_2$-type structure was reported at 641 nm under blue light (429 nm) excitation.[3] No studies have attempted to introduce the Eu^{2+} activator into ternary oxides with the same structure type. In the present study, single phase $NaLuO_2$ was synthesized from Na_2O and Lu_2O_3, and the preparation of Eu^{2+}-doped $NaLuO_2$ was attempted through the reaction of $NaLuO_2$ and EuO.

2. Experimental

The starting materials used were Na_2O (78.0–122.0 %, $Na_2O_2 \leq 22.0$ %, Sigma-Aldrich), Lu_2O_3 (99.9 %, High Purity Chemicals), Eu_2O_3 (99.9 %, Shin-Etsu Chemical Co. Ltd.), and Eu (99.9 %, Rare Metallic Co., Ltd.). Due to Na_2O, Eu, and EuO reacting with water vapor and oxygen in the air, the handling of these materials was carried out in a glove box filled with N_2 gas. For the synthesis of $NaLuO_2$, Na_2O and Lu_2O_3 were weighed at a molar ratio of 1.1:1.0, mixed in an agate mortar, and then pressed into a disk shape compact with a diameter of 5 mm and a thickness of ~1 mm with a die and a hand pressing tool. The compact was placed in a boat made of thin Ni plate and sealed along with N_2 gas in a stainless-steel container (SUS316L) composed of a tube (inner diameter 10.7 mm, length 80 mm) and caps. The container containing the sample was heated in an electric furnace at 1150 °C for 0.5 h, then cooled at a rate of −100 °C/h until it reached 850 °C. Subsequently, the power supply to heater elements was stopped and the sample was cooled in the furnace (furnace cooling).

A mixture of Eu_2O_3 and Eu metal fragments was sealed in the stainless-steel container and heated at 800–900 °C for 24 h to prepare EuO.[19] The obtained $NaLuO_2$ and EuO were ground in an agate mortar, weighed to give a $NaLuO_2$-to-EuO molar ratio of 1:x % (x = 0.01, 0.1, 1.0), and mixed before being pressed into compact disks. The $NaLuO_2$–xEuO compacts were placed in the Ni boat, which was then sealed in the stainless-steel container and heated at 900 °C for 12 h. After furnace cooling, the container was opened in air, and the sample was pulverized in the agate mortar.

For the single-phase $NaLuO_2$ sample, the X-ray diffraction (XRD) pattern was measured using a powder X-

† Corresponding author: H. Yamane; E-mail: YAMANE.Hisanori@nims.go.jp
‡ Corresponding author: T. Takeda; E-mail: TAKEDA.Takashi@nims.go.jp

ray diffractometer (RIGAKU, SmartLab) with a Cu Kα_1 (45 kV, 200 mA) radiation source, and Rietveld analysis was performed using the PDXL software.[20] The crystal structure was drawn using VESTA.[21] The crystalline phases were identified and the cell parameters of the trigonal phase in the $NaLuO_2$–xEuO samples were measured using a powder X-ray diffractometer (RIGAKU, SmartLab) with parallel beam Cu Kα radiation (40 kV, 30 mA) for accurate cell parameters. Excitation and emission spectra of the powdered samples were measured using a fluorescence spectrofluorometer (JASCO, FP8600), and the quantum efficiency of the emission was measured using a quantum efficiency measurement system (Otsuka Electronics Co., Ltd., QE-2100).

3. Results and discussion

In the synthesis of $NaLuO_2$, trace Na metal deposit was characterized in the stainless-steel container after heating at 1150 °C. Excess Na_2O above the $NaLuO_2$ stoichiometric composition evaporated from the sample and was pyrolyzed or reduced to Na metal by the stainless steel. **Figure 1** shows the powder XRD pattern of the synthesized $NaLuO_2$. The Rietveld analysis results with the α-$NaFeO_2$-type crystal structure model are summarized in **Table 1**. All diffraction peaks could be indexed with the cell parameters of the hexagonal system [a = 3.33373(7) Å, c = 16.5494(4) Å]. These parameters are close to those reported by Blasse et al. (a = 3.32 Å, c = 16.52 Å),[9] Zaitsev et al. (a = 3.34 Å, c = 16.48 Å),[13] Spitsyn et al. (a = 3.222 Å, c = 16.495 Å),[11] Murav'eva et al. [a = 3.322(1) Å, c = 16.495(5) Å],[12] Hashimoto et al. [a = 3.3518(6) Å, c = 16.5300(12) Å],[17] and GuO et al. (a = 3.335 Å, c = 16.545 Å).[15] The only O site z coordinate to be refined, was 0.2397(3). This coordinate was consistent with the z of α-$NaFeO_2$-type oxides $NaErO_2$ [0.236(4)][17] and $KLnO_2$ (Ln = Y, Nd, Sm–Lu) [0.2248(5)–0.2337(9)],[18] and the z of S site for the sulfides $ALnS_2$ (A = K, Rb; Ln = La, Gd, Lu, Y) [0.2303(2)–0.23718(11)].[22,23] The crystal structure of $NaLuO_2$ refined by Rietveld analysis is shown in **Fig. 2**. The Na–O and Lu–O interatomic distances shown in the analysis were 2.471(4) and 2.273(3) Å, respectively. The bond valence sums calculated using the parameters presented by Brese and O'Keeffe[24] were 0.979 and 2.654 for the Na and Lu sites, respectively, which are close to the Na and Lu oxidation numbers I and III, respectively.

The powder XRD pattern of the $NaLuO_2$–xEuO samples with the parallel beam geometry are shown in **Fig. 3**. Trace Lu_2O_3 XRD peaks of 222 and 400 were observed at 2θ = 29.69 and 34.43°, respectively, in the samples of x = 0.01, 0.1, and 1.0 %. **Figure 4** shows the cell parameters a and c and volume V of the trigonal phase normalized by the x = 0 % values. Cell parameters and volumes were slightly smaller for the x = 0.01 and 0.1 % samples compared with those of the x = 0 % sample but exceeded those for the x = 1.0 % sample. A trace Na metal deposition was identified in the stainless-steel container in which the $NaLuO_2$–xEuO samples were synthesized. The Lu_2O_3 XRD peak intensity from the x = 1.0 % sample was the highest, suggesting the Na_2O component was reduced in the reaction between $NaLuO_2$ and EuO, becoming Na vapor and being released from the sample. Some of the Eu^{2+} was oxidized and incorporated into $NaLuO_2$ as Eu^{3+}, and the excess Lu_2O_3, which became redundant owing to the loss of Na_2O and Eu^{3+} substitution, was expelled.

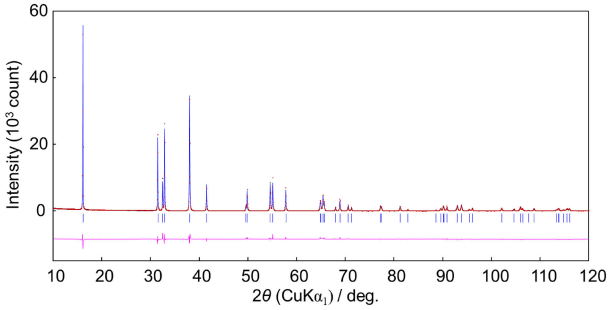

Fig. 1. Observed (dots) and calculated (solid) X-ray diffraction profiles for $NaLuO_2$. Tick marks below the diffraction pattern represent the allowed Bragg reflections. The difference profile is located at the bottom of the figure.

Table 1. Crystallographic data and structure refinement for $NaLuO_2$

Formula				$NaLuO_2$	
Formula weight				229.956	
Space group				trigonal, $R\bar{3}m$ H (166)	
Radiation wavelength				1.540593 Å (Cu Kα_1)	
Cell parameters				a = 3.33373(7) Å, c = 16.5494(4) Å	
Cell volume				V = 159.285(6) Å^3	
Density (calculated)				7.19 g/cm^3	
R indexes				R_{wp} = 9.70 %, R_p = 7.64 %, R_{exp} = 4.65 %	
Goodness of fit				S = 2.0855	
Atomic coordinates and isotropic displacement parameters					
Atom	Site	x	y	z	U_{iso} (Å^2)
Na	3a	0	0	0	0.0097(12)
Lu	3b	0	0	1/2	0.0018(2)
O	6c	0	0	0.2397(3)	0.0015(13)

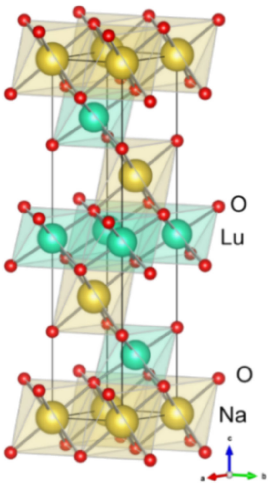

Fig. 2. Crystal structure of $NaLuO_2$.

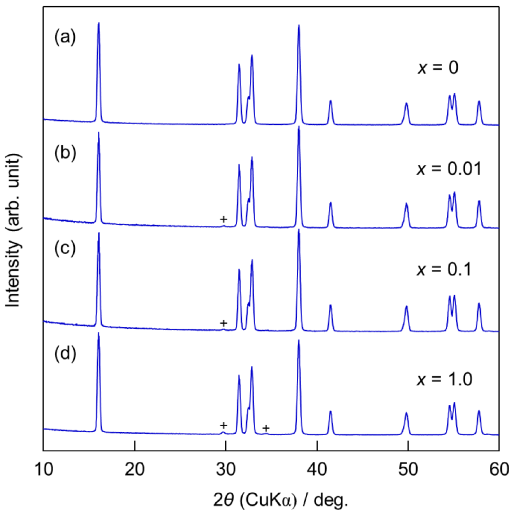

Fig. 3. X-ray diffraction patterns of the $NaLuO_2$–xEuO samples, (a) $x = 0$, (b) 0.01, (c) 0.1, and (d) 1.0. The peaks from Lu_2O_3 are indicated with "+".

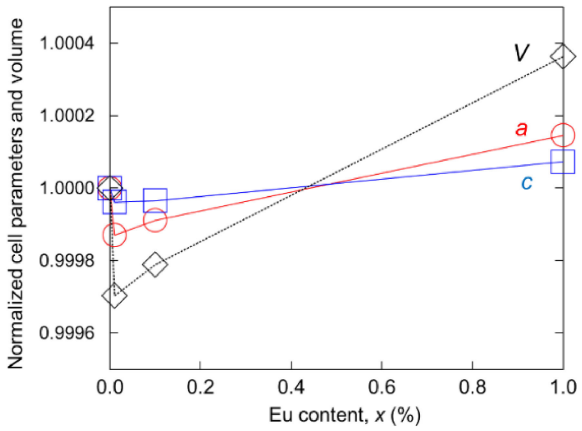

Fig. 4. Normalized hexagonal cell parameters (a, c) and volumes (V) for the trigonal phase in the $NaLuO_2$–xEuO samples ($x = 0$, 0.01, 0.1, and 1.0).

Figure 5 shows the excitation and emission spectra of the $x = 0.1$ % sample, in which 442 nm blue light excitation produced red emission from the $5d \rightarrow 4f$ transition of Eu^{2+} with a peak at 617 nm. The external and internal quantum efficiencies of this luminescence were 4.9 and 15.8 %, respectively. Compared to the emission peak at 641 nm and the excitation peak at 429 nm reported for $NaLuS_2$: 0.05 %Eu,[3] the emission peak wavelength was 24 nm shorter and the excitation peak wavelength was 13 nm longer for the $NaLuO_2$–xEuO samples. This is due to the difference in chemical bonding between the Eu–O and Eu–S in the crystals with the same structure type. The full width at half maximum (FWHM) of the emission peak estimated from the reported spectrum of $NaLuS_2$: 0.05 %Eu was 79 nm (0.24 eV),[3] which agreed with the FWHM of 80 nm (0.25 eV) for $NaLuO_2$–xEuO within the resolution of the spectrofluorometer. The sample was left in air for more than 2 weeks, but no change in the luminescence intensity or XRD pattern was observed.

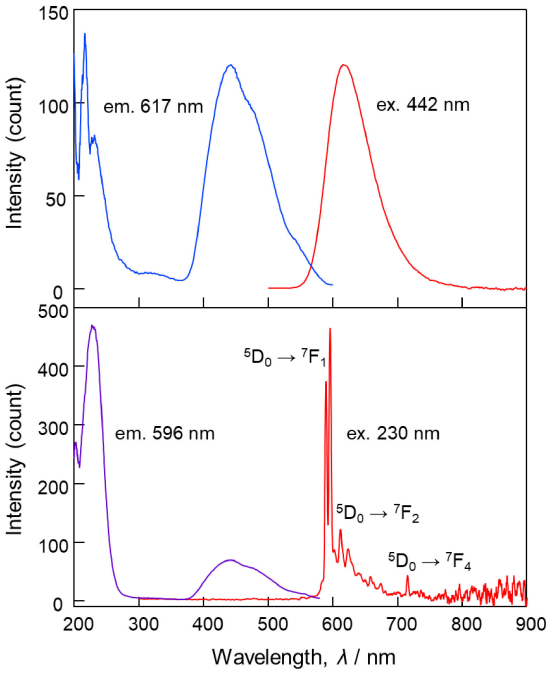

Fig. 5. Excitation and emission spectra measured for the $NaLuO_2$–0.1EuO sample at 25 °C.

Under UV light excitation with a 230 nm wavelength, an emission spectrum with the highest intensity peak at 596 nm caused by the $4f$–$4f$ transition ($^5D_0 \rightarrow {}^7F_1$) of Eu^{3+} was observed. This emission spectrum was also overlapped by a broad peak due to the $5d \rightarrow 4f$ transition of Eu^{2+}. At the excitation spectrum measured at 596 nm, an excitation band of Eu^{2+} with a peak at 442 nm appeared in addition to the charge transfer band at approximately 230 nm. Excluding the broad emission peak of Eu^{2+}, the Eu^{3+} emission spectrum was consistent with that of $NaLuO_2$:Eu^{3+} synthesized from Eu_2O_3.[14,15,25]

The emission peak intensity of Eu^{2+} was highest at $x = 0.1$ % and decreased at $x = 1$ % as shown in **Fig. 6**. In contrast, the intensity of Eu^{3+} at 596 nm increased with increasing x. In the isotypic Eu^{2+}-doped sulfide $KLuS_2$, a significant decrease in luminescence intensity (concentration quenching) was reported at Eu optimum concentrations from 0.01 to 0.5 % and above.[1] The $x = 1$ % sample of $NaLuO_2$–xEuO showed a decrease in intensity from the emission of Eu^{2+}, and the emission of Eu^{3+} was already dominant at $x = 0.1$ %. This suggests that there is a limit to the amount of Eu^{2+} introduced into $NaLuO_2$, which could be estimated to be less than 0.1 %.

Electron spin resonance (ESR) showed that Eu^{2+} was introduced at three centers, two of which were the K^+ and Lu^{3+} sites of $KLuS_2$.[2] In the case of $NaLuO_2$, the cell parameters and volumes of samples with $x = 0.01$ and 0.1 % were slightly smaller than those with $x = 0$ %. The effective ionic radii for six-fold configuration are 1.02, 0.861, 1.17, and 0.947 Å for Na^+, Lu^{3+}, Eu^{2+}, and Eu^{3+}, respectively.[26] If Eu^{2+} and Eu^{3+} occupy the Na^+ site and Lu^{3+} site, respectively, the cell parameters will increase. The decrease in cell parameters could be explained by the

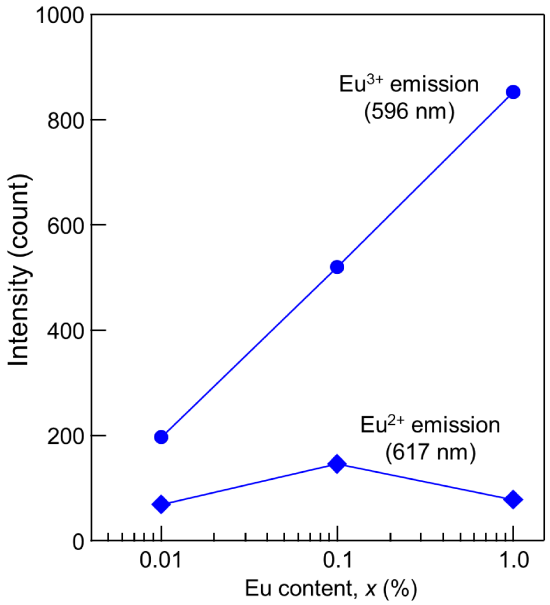

Fig. 6. Eu^{2+} and Eu^{3+} emission peak intensities observed for the spectra of the $NaLuO_2$–xEuO samples ($x = 0$, 0.01, 0.1, and 1.0).

occupation of the Na^+ site by both Eu^{2+}/Eu^{3+}. Thus, for the samples with $x = 0.01$ and 0.1 %, Eu^{2+} and Eu^{3+} might been introduced mainly at the Na^+ site, while for the $x = 1$ % sample, substitution of Eu^{3+} for Lu^{3+} at the Lu site proceeded, which increased the cell parameters and volume, leading to an increase in the Eu^{3+} emission intensity.

4. Summary

Single-phase $NaLuO_2$ with the α-$NaFeO_2$-type structure was synthesized by heating a mixture of Na_2O and Lu_2O_3 sealed with N_2 gas in a stainless-steel container at 1150 °C. Eu^{2+} doping of $NaLuO_2$ was attempted by heating the resulting $NaLuO_2$ with a variation of 0.01, 0.1, and 1.0 mol % EuO at 900 °C. The reaction of $NaLuO_2$ with EuO released Na and Lu_2O_3 and a part of Eu^{2+} was oxidized to Eu^{3+}. The amount of Eu^{2+} introduced into $NaLuO_2$ was estimated to be less than 0.1 mol %, and the peak emission of the $5d \rightarrow 4f$ transition of Eu^{2+} was observed at 617 nm under blue light excitation at 442 nm. The spectrum with the maximum intensity peak of Eu^{3+} emission at 596 nm under UV light excitation at 230 nm was consistent with that reported for Eu^{3+} doped $NaLuO_2$.

Acknowledgments This work was supported by JST, the Core Research for Evolutional Science and Technology (grant number JPMJCR19J2). It was also financially supported by the Innovative Science and Technology Initiative for Security (Grant Number JPJ004596, ATLA, Japan).

References

1) V. Jarý, L. Havlák, J. Bárta, E. Mihóková and M. Nikl, *Chem. Phys. Lett.* 574, 61 (2013).
2) V. Laguta, M. Buryi, L. Havlák, J. Bárta, V. Jarý and M. Nikl, *Phys. Status Solidi-R.* 08, 801 (2014).
3) V. Jarý, L. Havlák, J. Bárta, M. Buryi, E. Mihóková, M. Rejman, V. Laguta and M. Nikl, *Materials* 8, 6978 (2015).
4) V. Jarý, L. Havlák, J. Bárta, E. Mihóková, M. Buryi and M. Nikl, *J. Lumin.* 170, 718 (2016).
5) L. Havlak, V. Jary, J. Barta, M. Buryi, M. Rejman, V. Laguta and M. Nikl, *Mater. Design* 106, 363 (2016).
6) V. Jarý, L. Havlák, J. Bárta, M. Rejman, A. Bystřický, C. Dujardin, G. Ledoux and M. Nikl, *ECS J. Solid State Sc.* 7, R3182 (2018).
7) V. Jarý, L. Havlák, J. Bárta, M. Buryi, M. Rejman, M. Pokorný, C. Dujardin, G. Ledoux and M. Nikl, *ECS J. Solid State Sc.* 9, 016007 (2020).
8) M. G. Brik, V. Jarý, L. Havlák, J. Bárta and M. Nikl, *Chem. Eng. J.* 418, 129380 (2021).
9) G. Blasse, *J. Inorg. Nucl. Chem.* 28, 2444 (1966).
10) R. Hoppe and H. Sabrowsky, *Z. Anorg. Allg. Chem.* 339, 144 (1965).
11) V. I. Spitsyn, I. A. Murav'eva, L. M. Kovba and I. I. Korchak, *Zh. Neorg. Khim.* 14, 1451 (1969).
12) I. A. Murav'eva, L. M. Kovba and V. I. Spitsyn, *Dokl. Akad. Nauk SSSR* 172, 1380 (1967).
13) B. E. Zaitsev, B. N. Ivanov-Émin, V. M. Akimov, E. N. Siforova and V. Miliado Campos, *J. Struct. Chem.* 11, 634 (1971).
14) G. Blasse and A. Bril, *J. Chem. Phys.* 45, 3327 (1966).
15) R.-W. Guo, C.-X. Guo and D. Wu, *Acta Phys.-Chim. Sin.* 57, 607 (2008).
16) A. C. Van der Steen, J. J. A. Van Hesteren and A. P. Slok, *J. Electrochem. Soc.* 128, 1327 (1981).
17) Y. Hashimoto, M. Wakeshima and Y. Hinatsu, *J. Solid State Chem.* 176, 266 (2003).
18) B. Dong, Y. Doi and Y. Hinatsu, *J. Alloy. Compd.* 453, 282 (2008).
19) K. Hirose, Y. Doi and Y. Hinatsu, *J. Solid State Chem.* 182, 1624 (2009).
20) PDXL Version 2.8.4.0 (2017), Integrated X-ray Powder Diffraction Software. Rigaku Corporation, Tokyo 196-8666, Japan.
21) K. Momma and F. Izumi, *J. Appl. Crystallogr.* 44, 1272 (2011).
22) J. Fabry, L. Havlak, M. Dusek, P. Vanek, J. Drahokoupil and K. Jurek, *Acta Crystallogr. B* 70, 360 (2014).
23) W. Bronger, J. Eyck, K. Kruse and D. Schmitz, *Eur. J. Sol. State Inor.* 33, 213 (1996).
24) N. E. Brese and M. O'Keeffe, *Acta Crystallogr. B* 47, 192 (1991).
25) G. Blasse and B. C. Grabmaier, "Luminescent Materials", Springer-Verlag, Berlin (1994) p. 43.
26) R. Shannon, *Acta Crystallogr. A* 32, 751 (1976).